

Design and control of an ambidextrous robotic hand

Rafael Cathomen, Matthias Jammot, Timothée Joguet, Mario Müller, Tim Vaughan-Whitehead

Abstract—In the realm of robotic hand design, the prevailing state-of-the-art primarily focuses on mimicking human-like capabilities, often constrained by a balance between complexity, weight, and functionality. With this work, we introduce a novel robotic hand design that transcends these limitations. Our design follows a non-anthropomorphic approach, notably featuring a four degree of freedom thumb, which considerably enhances dexterity and manipulation capabilities. The hand’s mechanical structure, consisting of a unique finger configuration with rolling contact and pin joints, along with a high-friction silicone skin and a 3D-printed concave palm, in combination with reinforcement learning, enables versatile and effective object manipulation. Our experiments demonstrate the hand’s proficiency in simulated tasks like sphere rotation and real world applications like teleoperated object handling. Despite challenges in the Sim2Real transfer, the results showcase the potential of our design in achieving greater dexterity and functionality in robotic hands.

I. INTRODUCTION

A. Motivation

With the ongoing progress in robotics, the demand for different grippers tailored to varying tasks has been rapidly increasing. While grippers for simple repetitive tasks have become ubiquitous, such as the picking and placing of objects, only a few solutions provide adaptability to diverse and complex tasks. With robotics expanding to human everyday life applications, versatile hand grippers have become increasingly researched. Most hand grippers have inferior or equal numbers of fingers, joints, and therefore degrees of freedom than a human hand, allowing them to perform at best human-like tasks [1]. Such design considerations exist due to a trade-off between the system’s complexity, capability, reliability, weight, and cost [2].

In this paper, we address the need for hand grippers able to perform various difficult tasks, by proposing a novel tendon-driven hand. Our design is shown in Figure 1. Tendon actuation allows for smaller hand volumes by placing the servo motors outside the hand’s active envelope. An intricate routing of the tendon has to be devised to maximize the transmission’s efficiency. By coupling the agonist and antagonist tendons of all joints, our hand only requires eleven motors, making it light and affordable. Four degrees of freedom in the thumb and three in the pinky allow for a high adaptability to various shapes and help with more challenging tasks such as in-hand manipulation. Partnered with these mechanical advances, control methods, such as learning-based control and teleoperation, are implemented to extend the utility of our robotic hand to a wider range of applications.

The versatility demonstrated in our ambidextrous hand benefits human-like interactions by being more mechanically,

financially, and computationally cost-effective. Its ability to switch from a right to a left hand allows it to navigate in a more optimized manner and confined space, not requiring any major adjustments in the robotic arm’s configuration it is attached to. An example of this would be in agriculture when harvesting crops, adapting to the different orientations and placements of crops effortlessly. Similarly, manipulating different tools and objects, such as in a logistical, manufacturing, or surgical setting, would be more time efficient. Finally, human-robot interactions would be enhanced, like teleoperation for both right and left handed users.

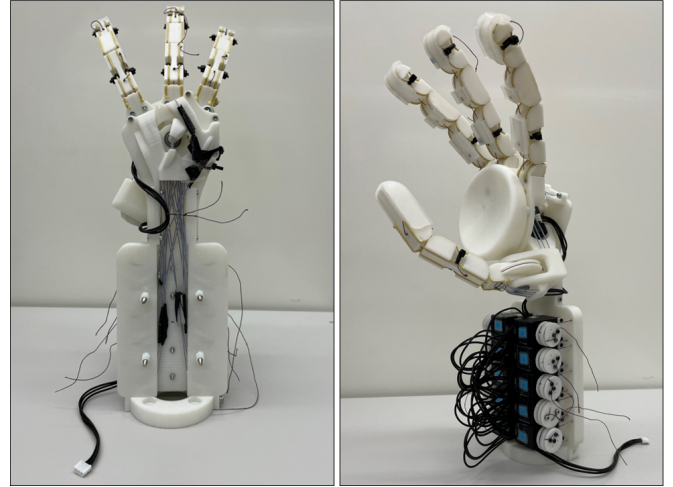


Fig. 1: Overview of the ambidextrous, compliant robotic hand, capable of dexterous manipulation.

B. Related Work

a) Robotic hand hardware: When it comes to robotic hands, most designs diverge depending on their application, such as on the number of fingers, the transmission method, and joint types. For example, Ottobock’s bebionic hand [3], designed for commercial applications for prosthetic users and therefore anthropomorphic in its shape, has five fingers, four of which have two pin joints with integrated rotational springs and a thumb with three joints. The fingers are actuated via a four-bar linkage system. On the other hand, the Faive hand [4], which is highly anthropomorphic as well with its five fingers, uses a tendon-driven transmission coupled with rolling contact joints. This mimics the muscles and fibers of hands by adding compliance. The DLR hand II [5] has four fingers with three degrees of freedom each, actuated via toothed belts, drive gears, and bevel gears. While this design choice provides a very precise kinematic control, it lacks in compliance, potentially hindering its ability in

dexterous manipulation tasks, and is especially heavy at 2.2 kg. The RTR-II hand [6], for simplicity and weight-saving purposes, has only three fingers. Those are flexed by a tendon-driven mechanism by means of small pulleys situated at each joint and extended with rotational springs, adding compliance.

b) Learning-based control: The two main learning-based control methods in dexterous manipulation are model predictive control (MPC) and reinforcement learning (RL). MPC is an optimization of the system's dynamics to predict its future behavior over a finite time horizon, whereas RL is machine-learning based and optimizes a control policy to fit an intended outcome. Although RL requires no knowledge of the system in comparison to MPC, it is less sample-efficient due to requiring more data and being unable to exploit real-world data optimally. [7] developed an MPC to optimize the impedance parameters for compliant robotic manipulation, which proved more beneficial than model-free and model-based RL approaches in solving tasks without the need to relearn the model or policy. [8] developed a demonstration augmented policy gradient (DAPG) algorithm which combines reinforcement learning with imitation learning using the demonstration data for different robotic hand geometries. This reduced the learning time and improved the model's performance for a deep RL model on real hardware. [9] used imitation learning to track the motion of the object being manipulated by the RBO 2 hand [10], ran a selection process for the best demonstration, and applied RL to learn a policy that optimizes their controllers. This method enabled successful manipulation of dexterous tasks, such as turning valves, moving beads, and grasping objects. Some research investigated the merging of both those methods [11], leveraging RL's strength in exploration to better train the forward dynamics model fed in to the MPC. While RL and MPC are very promising for dexterous manipulation, they face some limits, such as the Sim2Real gap, which describes the learned policy's inability to exactly match the simulation's performance in the real world due to differences between the simulated environment and the real world.

C. Contribution

The contributions of this work are:

- A non-anthropomorphic hand design with an ambidextrous four degree-of-freedom thumb and three degree-of-freedom pinky finger.
- An efficient tendon routing via polytetrafluoroethylene (PTFE) tubes, reducing the friction in the tendons, simplifying the design complexity, and increasing the control accuracy by limiting cable stretching.
- The implementation of hand-tracking-based teleoperation tailored to a non-anthropomorphic robotic hand.
- Training of reinforcement learning policies to rotate a sphere about different axes in simulation and applying the trained policies to the hand.

II. HARDWARE DESIGN

A. Finger configuration

The aim of our hand design was to enable dexterous object manipulation by introducing novel features. Faced with a constraint of having only 11 motors, the robotic hand was designed with four fingers, thereby enhancing the available degrees of freedom per finger compared to a more anthropomorphic five-fingered hand. A major decision was to allocate four degrees of freedom to the thumb for an increased versatile functionality, in particular for tasks such as grasping and object manipulation. The index and middle finger have three rolling contact joints each. Their last two joints are coupled, creating a two degrees of freedom linkage. The pinky finger contains an additional abduction joint, implemented as a pin joint. The finger configuration is shown in Figure 2. The hand displays ambidextrous capabilities provided by the thumb's large range of motion, allowing it to be easily converted from a right hand to a left hand should the task require it.

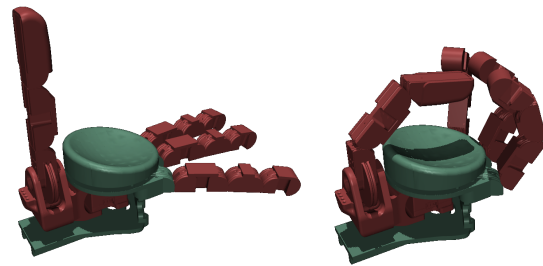


Fig. 2: Robotic hand in open and half-closed configurations.

B. Four degrees of freedom thumb

The key innovation in our robotic hand lies in the incorporation of a four degrees of freedom thumb, a feature that significantly enhances the hand's versatility and adaptability. This original design is characterized by two pin joints, the first of which is located below the center of the palm and is actuated in a direct drive fashion. The second pin joint is perpendicular to the palm and allows the thumb to tilt sideways. These two unusual ranges of motion are displayed as a motion trail in Figure 3.

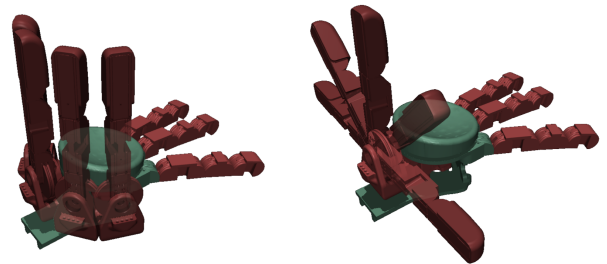


Fig. 3: Motion trail of the first thumb joint (left), and of the second thumb joint (right).

C. Joint selection

The two types of joints used were pin joints and rolling contact joints. All outer joints of the fingers are rolling contact joints of rolling radius 1 cm. This offers a favorable compromise in maintaining a small form factor while still being large enough to have significant tendon length changes required for precise control and high joint torques. Rolling contact joints were selected for their ease of manufacture and assembly, high strength, and low friction. The performance of the rolling contact joints is, however, highly dependent on the ligament tension. The ligament's elongation over time and the generated slack during assembly hinder the joint's robustness. In order to address this issue, Kevlar ligaments were selected for their resistance to elongation, wear and abrasion, whilst remaining highly flexible. In addition, the fingers were designed with cutouts for cable ties to adjust ligament tension after assembly, as shown in Figure 5. Pin joints in the pinky abduction and the first two thumb joints were selected for their small footprint, the constant center of rotation, and their compatibility with direct drive actuation.

D. Actuation

The fingers are tendon-actuated, allowing greater spatial freedom, high force transmission, and compliance. All joints are actuated by an antagonistic tendon pair, driven by a Dynamixel XC330-T288-T. The agonist-antagonist tendon scheme, which minimizes the number of motors used, is exemplified in Figure 5. The antagonist spools are mounted onto the agonist spools with rotational springs situated in between them, as displayed in Figure 4.

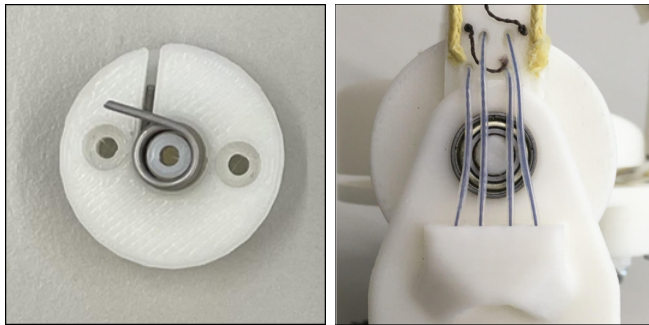


Fig. 4: Torsional spring situated between the agonist and antagonist spools to provide joint extension and compliance (left), PTFE tubes carrying tendons to simplify tendon routing by keeping a constant tendon length (right).

Consequently, finger positions are controlled over the length of the agonist tendon, whereas the antagonist tendon is tensioned by the torsional spring, allowing the hand to open if the agonist tendon is extended and preventing the build-up of slack. The spools of the tendon driven pin joints do not require any spring since the tendon length of agonist and antagonist is exactly the same. A braided fishing line is used for the tendons due to its high strength, flexibility, and minimal stretching. If a higher compliance were desired, a more flexible monofilament fishing line could be selected, at the cost of control accuracy. PTFE tubes in which the

cables slide simplify the tendon routing, reducing the cable's friction with its surroundings, allowing for sharper turns and maintaining a constant tendon length within the tube. This is required in situations where the tendons cannot be routed internally, as displayed in Figure 4.

E. Skin and Palm

The deliberate choices in skin and palm design contribute to the overall functionality and adaptability of the robotic hand. For the skin, high friction silicone was crafted through casting. The skin enhances the hand's gripping capabilities, as the soft surface provides increased friction and compliance, enabling a more secure hold on objects. The skin was attached only on one side of the fingers, except for the tip of the thumb, as may be seen in Figure 5. In tandem with the silicone skin, the palm design is a well-thought element of the hardware configuration. The palm's concave shape resembles that of a human palm. The concave design of the palm proved to be especially advantageous in preventing the inadvertent displacement of objects, particularly those with a tendency to roll or slide. This feature is particularly beneficial when handling spherical objects, as the concave curvature cradles and stabilizes them, minimizing the risk of accidental drops. Another noteworthy feature is its modularity, allowing for easy replacement or modification as needed. This flexibility enables the adaptation of different palm shapes to suit specific tasks or preferences.

F. Modeling and low level control

The robotic hand's kinematics proved to be a fundamental component in its control strategy for achieving precise control. The conversion from changes in tendon length, induced directly by the motor, to corresponding joint angles, forms the cornerstone of the approach taken for the hand's control, enabling a seamless translation from desired hand positions to the necessary motor adjustments.

III. CONTROL STRATEGIES FOR MANIPULATION

To control the robotic hand, we employed two different approaches, hand-tracking-based teleoperation and reinforcement learning for autonomous object manipulation.

A. Teleoperation

To operate the robotic hand, the Luxonis OAK-D Pro¹ stereo camera was used to capture the human hand with a deep learning algorithm [12] to detect the 3D positions of all joints. To map the detected joint positions to the joint angles of the robot hand, an angle-based approach was adopted, mapping the angles between corresponding points on the human hand to the robotic hand. One notable consideration arose in the case of the thumb, which inherently possesses a greater range of motion than a human hand. To navigate this challenge, we introduced various prefixed positions for the first degree of rotation around the palm. This innovation enhanced the versatility of the teleoperation, dynamically

¹<https://docs.luxonis.com/projects/hardware/en/latest/pages/DM9098pro/>

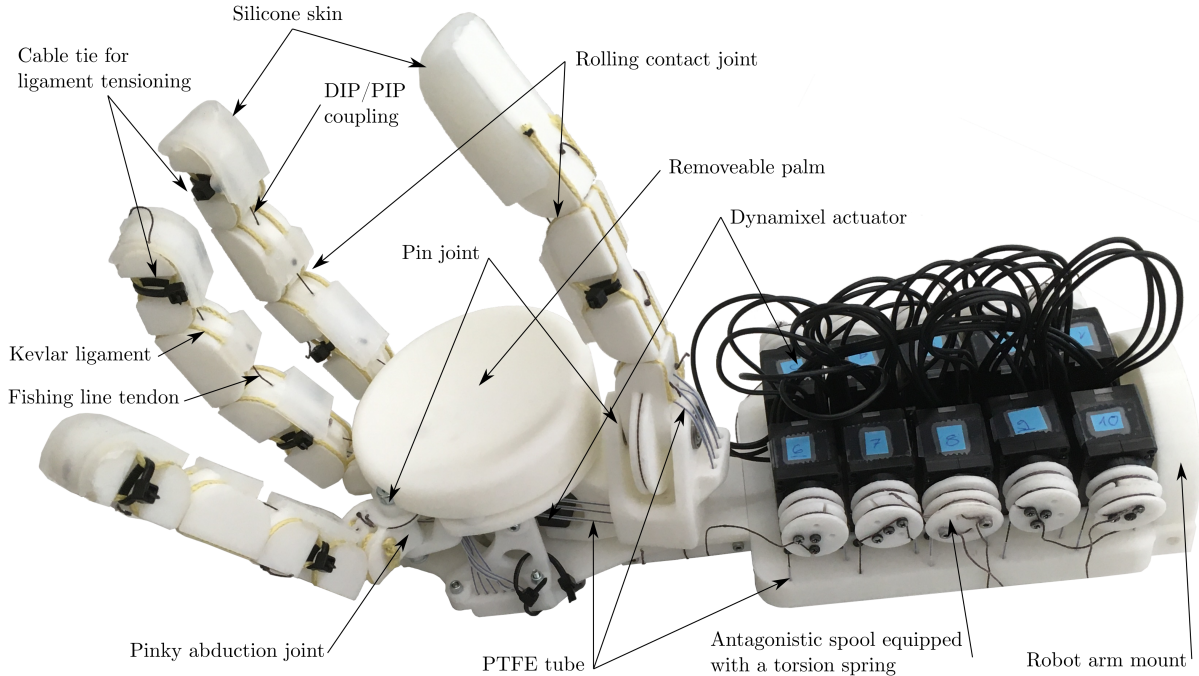


Fig. 5: Robotic hand assembly: All non standard parts are manufactured using a 3D printer (white parts in the image). The ligaments are glued to the 3D printed parts and tightened with the cable ties. All components of the palm and of the motor pack are mounted with bolts and nuts. The spools consist of two parts, connected with a torsional spring. The flexor tendon is directly driven, while the extensor tendon is coupled with the torsional spring.

adjusting the thumb’s positioning to facilitate specific tasks. For instance, these prefixed positions proved beneficial in optimizing the hand’s ability to pinch or grasp objects with different fingers during teleoperation. This teleoperation strategy, rooted in deep learning and thoughtful angle mapping, contributes to the seamless integration of human-like movements in the robotic hand, paving the way for intuitive and precise control.

B. Reinforcement learning

To showcase the hand design’s versatility, a 10 cm diameter sphere was rotated in various directions using RL. The RL pipeline from [4] served as a foundational basis, essentially using the PPO algorithm [13] implemented by the open-source repository *rl_games* [14] and using Isaac-Gym [15] as the simulator. If not mentioned otherwise, our implementation is the same as in [4]. Since no proprioceptive sensing was implemented on the hardware side, except for the encoders measuring joint angles inside the servos, it would be difficult to do any kind of manipulation because no observations of the manipulated object were available. Therefore, we recorded trained policies in simulation and played them back on the real system. For the task of rotating a sphere, which is symmetric about all its axes, the sphere’s orientation does not influence how the hand interacts with it. This justified simplifying the training pipeline by using the same observations for actor and critic, which are the union of the actor and critic observations, described in [4]. We also employed domain randomization to mitigate inaccuracies inherent in the physics simulation, thereby proactively

reducing the discrepancies in the Sim2Real gap. Table I lists the rewards used for the task and their formula. The reward function is parameterized by a unit vector \mathbf{n} , which indicates the desired direction of rotation. The reward is scaled linearly with the rotational velocity up to a maximum of 3 rad/s. The direction of the angular velocity is rewarded by projecting it normalized on to \mathbf{n} and exponentiating this by a squashing constant, in our case 8.

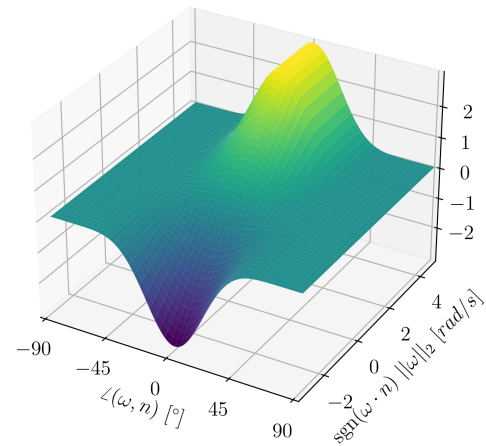


Fig. 6: Object rotation reward surface

Figure 6 plots the surface of the reward for the rotation. As in [4], we used the numerical differentiation of the object orientation instead of using the angular velocity by IsaacGym. Dropping the object and high torques were penalized. This

Reward	Formula	Weight	Justification
Object rotation	$\text{sgn}(p) p ^8 \min(\omega _2, 3), p = \mathbf{n} \cdot \frac{\omega}{ \omega _2}$	0.01	Reward the rotation about an arbitrary unit vector \mathbf{n}
Torque penalty	$ \tau _2$	-0.01	Prevent joints from applying large torques
Drop penalty	$ \mathbf{x}_{obj} - \mathbf{x}_{hand} _2 > 30 \text{ cm}$	-1.0	Penalize object drops

TABLE I: Rewards and penalties used during training.

approach led to one policy per desired direction of rotation. These policies could be combined into one, by randomly changing \mathbf{n} during training and enabling the agent to observe it. When training such a policy, we noticed a more than tenfold slower convergence. Since we wanted to showcase the viability of the mechanical design, we decided against this approach, as from a mechanical perspective, it did not matter if there was one policy per direction or one for all.

IV. EXPERIMENTS AND RESULTS

A. Teleoperation

Our approach with the prefixed positions worked especially well for pinch grasps, which enabled the operator to grab a variety of different objects, including a cube, an apple, a mug, a piece of paper, a fidget spinner, and a plush animal. Power grasping objects also worked, but only if the object was big enough. Since our robot hand is very different from a human hand, the teleportation is not as intuitive as it could be for an anthropomorphic robot hand. However, after a few minutes of learning, everyone in our team was able to operate the hand.

B. Rotating the sphere with reinforcement learning

We trained six different policies, all with the same setup but with different desired rotation directions. In simulation, the palm was pointing upwards, but tilted 20° forwards, such that in a fully extended configuration, the ball would roll from the palm to the middle finger and then fall down. For the desired axes of rotation, we chose the positive and negative directions of the x , y and z axes of the world frame of the simulator. Figure 7 indicates that the best performing policy for each direction achieved an absolute angular velocity of more than 1 rad/s, which is roughly what was achieved by [4]. Also noteworthy is the high variance in the different runs, suggesting that doing multiple runs with different seeds is crucial to get representative performances of the RL setup. The current joint configuration of the thumb favors rotation about the z -axis, as the best policy in this direction achieves an angular velocity above 2 rad/s. When rolling out these policies on the real robot, the performance was drastically reduced. The z direction worked, in the sense that the sphere was visually rotating, but the opposite $-z$ direction did not work at all. We believe this is due to the Sim2Real gap, which in our case was particularly significant.

C. Mechanical Design

a) *Design:* Since the design is not a result of a mathematical optimization, we cannot say that it is optimal in any way, but the chosen finger configuration enabled the hand to grasp different objects and was able to rotate a

sphere in all directions in simulation. This indicates the current design is viable for the chosen applications. When testing the grasping of different objects, we noticed that our hand was considerably bigger than a normal human hand. Also, the hand cannot enter a fully closed configuration resembling a fist. As a result of that, our hand cannot grab thin objects using a power grasp, like a pen or a mug handle. Nevertheless, thanks to the highly dexterous thumb, we were able to perform proper pinch grasps between the thumb and any other finger, which enabled us to grasp small objects.

b) *Hardware Implementation:* The key difference between our implementation and [4] was the usage of PTFE tubes to guide the tendons. The tubes were used to provide a bendable tendon guide with low friction. Even though the tendon guide to the thumb joints was highly curved at multiple points, we never encountered issues due to friction loss or changes in length induced by joint rotations, thanks to the low friction coefficient of PTFE and efficient tendon routing. We also noticed, that the tubes we used could crumble under maximum load, altering the tendon's length at the joint, thus defeating the main purpose of using tubes. We accounted for this by limiting the maximum force. A better way to account for this would be to use thicker tubes. Using cable ties to tighten the ligaments proved to be a double-edged sword; they properly tightened the ligaments, resulting in a smooth rolling contact joint, but slightly misaligned the joints, which significantly contributed to the Sim2Real gap when transferring the RL policies.

V. CONCLUSION

In this work, we introduced a novel non-anthropomorphic robotic hand design which outperforms common robotic hands at certain tasks, while not requiring additional degrees of freedom. This was achieved by increasing the dexterity and versatility of the thumb. The thumb consists of four joints, each with a high range of motion. Due to the high discrepancy between a human hand and our robotic hand, we developed a unique teleoperation interface, which enabled a human user to operate the robot hand with their own hand. The mapping between the tracked joints of the human hand and those of the robotic hand allowed the user to grasp different objects such as a mug, a plush animal, an apple or a piece of paper. To further demonstrate the capabilities of our hand's design, we trained reinforcement learning policies for a variety of tasks. This showed that our hand was capable of rotating a sphere about all coordinate axes with a rotational speed of more than 1 rad/s. Due to the significant Sim2Real gap, likely stemming from small joint misalignments, we were not able to transfer all trained policies successfully to the real robot. In future work, more care should be taken to

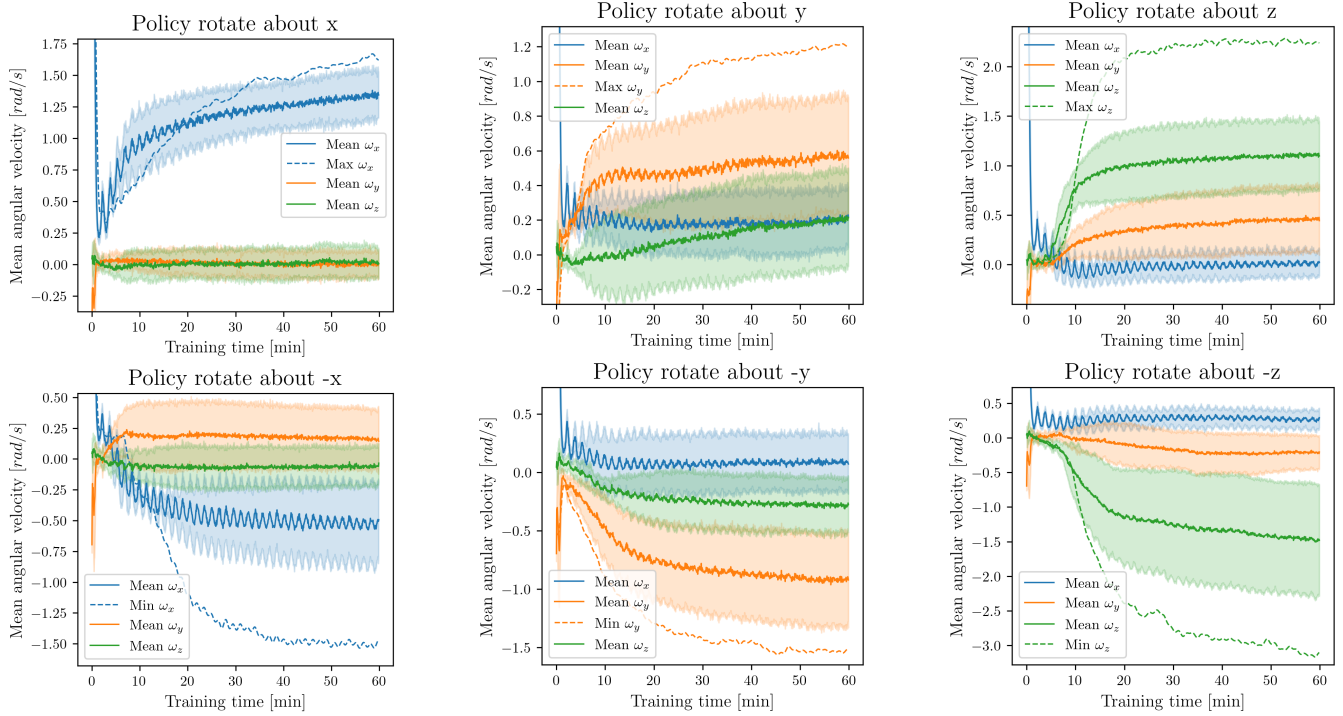


Fig. 7: Evolution of the average angular velocity of the sphere for six different policies. We took the mean of 15 training rounds for each policy. An area of $\pm\sigma$ is shown around the mean curve. The dashed line indicates the angular velocity of the best performing of the 15 policies.

properly align all joints to minimize the Sim2Real gap. Since we limited our policy training to sphere rotation, future work should focus on expanding the hand's capabilities by training policies on a wider range of tasks. Our hand design, not being the result of an optimization, can be improved, ideally by jointly optimizing the control policy and the physical design with regards to a wide range of tasks.

ACKNOWLEDGMENTS

We would like to thank the Soft Robotics Lab at ETH Zurich and all teaching assistants of the “Real World Robotics” course for providing access to their cutting-edge facilities, for their funding, and most importantly for their invaluable support and expertise.

REFERENCES

- [1] A. Vazhapilli Sureshbabu, G. Metta, and A. Parmiggiani, “A systematic approach to evaluating and benchmarking robotic hands—the ffp index,” *Robotics*, vol. 8, no. 1, 2019. [Online]. Available: <https://www.mdpi.com/2218-6581/8/1/7>
- [2] M. Chalon, A. Wedler, A. Baumann, W. Bertleff, A. Beyer, J. Butterfaß, M. Grebenstein, R. Gruber, F. Hacker, E. Krämer, K. Landzettel, M. Maier, H.-J. Sedlmayr, N. Seitz, F. Wappler, B. Willberg, T. Wimböck, G. Hirzinger, and F. Didot, “Dexhand : a space qualified multi-fingered robotic hand,” in *Proceedings*, May 2011. [Online]. Available: <https://elib.dlr.de/74368/>
- [3] Ottobock. (Accessed 2024) 8E70 - Product Information. [Online]. Available: <https://www.ottobock.com/en-ex/product/8E70>
- [4] Y. Toshimitsu, B. Forrai, B. G. Cangan, U. Steger, M. Knecht, S. Weirich, and R. K. Katzschmann, “Getting the ball rolling: Learning a dexterous policy for a biomimetic tendon-driven hand with rolling contact joints,” 2023.
- [5] J. Butterfass, , and O. Authors, “DLR-Hand II: Next generation of a dexterous robot hand,” in *Proc. of the 2001 IEEE International Conference on Robotics and Automation (ICRA)*, Seoul, Korea, May 2001, pp. 109–114.
- [6] L. Zollo, S. Roccella, R. Tucci, B. Siciliano, E. Guglielmelli, M. C. Carrozza, and P. Dario, “Biomechatronic design and control of an anthropomorphic artificial hand for prosthetics and robotic applications,” in *Proc. of the 1st IEEE/RAS Int. Conf. on Biomedical Robotics and Biomechatronics, BioRob 06*, Pisa, Italy, February 2006.
- [7] A. S. Anand, J. T. Gravdahl, and F. J. Abu-Dakka, “Model-based variable impedance learning control for robotic manipulation,” *Robotics and Autonomous Systems*, vol. 170, p. 104531, Dec. 2023. [Online]. Available: <http://dx.doi.org/10.1016/j.robot.2023.104531>
- [8] H. Zhu, A. Gupta, A. Rajeswaran, S. Levine, and V. Kumar, “Dexterous manipulation with deep reinforcement learning: Efficient, general, and low-cost,” 2018.
- [9] A. Gupta, C. Eppner, S. Levine, and P. Abbeel, “Learning dexterous manipulation for a soft robotic hand from human demonstration,” 03 2016.
- [10] R. Deimel and O. Brock, “A novel type of compliant and underactuated robotic hand for dexterous grasping,” *The International Journal of Robotics Research*, vol. 35, no. 1-3, pp. 161–185, March 2016.
- [11] M. Omer, R. Ahmed, B. Rosman, and S. F. Babikir, “Model predictive-actor critic reinforcement learning for dexterous manipulation,” in *2020 International Conference on Computer, Control, Electrical, and Electronics Engineering (ICCCEEE)*, 2021, pp. 1–6.
- [12] geaxgx, “DepthAI Hand Tracker,” <https://github.com/geaxgx/depthai-hand.tracker>, 2023.
- [13] J. Schulman, F. Wolski, P. Dhariwal, A. Radford, and O. Klimov, “Proximal policy optimization algorithms,” July 2017.
- [14] D. Makoviychuk and V. Makoviychuk, “rl-games: A high-performance framework for reinforcement learning,” <https://github.com/Denys88/rl-games>, May 2021.
- [15] V. Makoviychuk, L. Wawrzyniak, Y. Guo, M. Lu, K. Storey, M. Macklin, D. Hoeller, N. Rudin, A. Allshire, A. Handa, and Gavriel State, “Isaac gym: High performance GPU based physics simulation for robot learning,” Nov. 2021.